Chemistry & Biology
Article

Structure-Guided Design of Fluorescent *S*-Adenosylmethionine Analogs for a High-Throughput Screen to Target SAM-I Riboswitch RNAs

Scott F. Hickey[1,3] and Ming C. Hammond[1,2,3,*]
[1]Department of Chemistry, University of California, Berkeley, CA 94720, USA
[2]Department of Molecular and Cell Biology, University of California, Berkeley, CA 94720, USA
[3]Synthetic Biology Institute, University of California, Berkeley, Berkely, CA 94720, USA
*Correspondence: mingch@berkeley.edu
http://dx.doi.org/10.1016/j.chembiol.2014.01.004

SUMMARY

Many classes of *S*-adenosylmethionine (SAM)-binding RNAs and proteins are of interest as potential drug targets in diverse therapeutic areas, from infectious diseases to cancer. In the former case, the SAM-I riboswitch is an attractive target because this structured RNA element is found only in bacterial mRNAs and regulates multiple genes in several human pathogens. Here, we describe the synthesis of stable and fluorescent analogs of SAM in which the fluorophore is introduced through a functionalizable linker to the ribose. A Cy5-labeled SAM analog was shown to bind several SAM-I riboswitches via in-line probing and fluorescence polarization assays, including one from *Staphylococcus aureus* that controls the expression of SAM synthetase in this organism. A fluorescent ligand displacement assay was developed and validated for high-throughput screening of compounds to target the SAM-I riboswitch class.

INTRODUCTION

Riboswitches are structured RNA elements typically found in bacterial mRNA untranslated regions that are capable of sensing cellular metabolites (Breaker 2011). Binding of the cognate ligand to the riboswitch aptamer domain affects a conformational change in the expression platform, resulting in regulation of downstream gene expression. To date, more than 20 classes of natural riboswitches have been discovered (Serganov and Nudler, 2013) that bind a wide variety of metabolites. These metabolites range in structure from simple amino acids such as glycine, to large and elaborate cofactors such as adenosylcobalamin, to the fluoride ion. The diversity of riboswitch ligands reveals the intrinsic potential of structured RNA elements to form binding pockets for specific molecular recognition.

Due to their roles in bacterial gene regulation and prospects of targeting the ligand binding pocket of the aptamer domain, riboswitches have generated interest for the development of novel antibiotics (Blount and Breaker, 2006; Deigan and Ferré-D'Amaré, 2011). Subversion of the normal regulatory response of the riboswitch by an exogenous compound may disable the function of essential genes and slow bacterial growth. The availability of ligand-bound crystal structures for many riboswitch classes has made it possible to identify ligand analogs by structure-based rational design (Deigan and Ferré-D'Amaré, 2011). For example, bactericidal compounds have been identified that target the lysine riboswitch (Blount et al., 2007; Budhathoki et al., 2012) and guanine riboswitch (Kim et al., 2009; Mulhbacher et al., 2010). Computational docking also has been used to predict new ligands for the guanine riboswitch; however, there is not a strong correlation between docking score and ligand affinity (Daldrop et al., 2011).

Alternatively, the development of high-throughput screening methods offers a separate approach for riboswitch ligand discovery. High-throughput methods allow rapid screening of more diverse sets of compounds, enabling discovery of candidate leads that would not be predicted by rational design. In addition, this approach takes advantage of the large and diverse chemical compound libraries that are available. Both fluorescence polarization and FRET-based assays have been developed for screening activators of the *glmS* riboswitch using fluorescently tagged oligonucleotides (Mayer and Famulok, 2006; Blount and Breaker, 2006). These screening techniques take advantage of the natural self-cleaving ability of the *glmS* ribozyme; however, they are limited by slow ribozyme kinetics and false-positive results from ligand-independent cleavage (de Silva and Walter, 2009). Although an allosteric ribozyme was engineered for the Vc2 c-di-GMP riboswitch to develop a similar screening assay (Furukawa et al., 2012), the method requires extensive optimization for each riboswitch sequence of interest.

Other screening techniques have been developed for riboswitches that do not have ribozyme activity. An equilibrium dialysis assay was used to screen a library of 1300 fragments for activity against the *Escherichia coli thiM* TPP riboswitch (Cressina et al., 2011; Chen et al., 2010). However, the method requires tritium-labeled thiamine and the fragments were screened in sets of five to increase throughput, necessitating an additional deconvolution step after the initial screen. We recently have described the development of a microfluidics-based mobility shift assay that has promising quantitative analytical capabilities in addition to being time and resource sparing (Karns et al., 2013). Adaptation of this technology to a multiplex format would be highly desirable for high-throughput screening.

Recently, a dual molecular beacon assay was described for the *Bacillus subtilis pbuE* adenine riboswitch in which ligand

analogs were screened for their ability to regulate transcription (Chinnappan et al., 2013). In contrast to other methods, this system enables cotranscriptional screening of ligand analogs in a functional context, which is important as kinetic parameters are known to be critical for riboswitch function (Wickiser et al., 2005). Thus, this method identifies compounds that not only bind the riboswitch aptamer, but also affect the transcriptional regulatory activity of the riboswitch. Although this assay has been demonstrated only in a low-throughput format, the technique is potentially amenable to high-throughput screening. However, optimization of the molecular beacons for each individual riboswitch sequence is still required and compounds with intrinsic fluorescence, transcriptional inhibitory activity, or that affect the molecular beacons themselves must be avoided (Chinnappan et al., 2013).

SAM-binding riboswitches have been largely unexplored as targets for novel antibiotics, even though seven different classes have been reported (SAM-I through SAM-V, SAM-I/IV, and SAM/SAH) that each have distinct structural features (Wang and Breaker, 2008; Batey 2011). These riboswitches have been extensively characterized both structurally (Baird and Ferré-D'Amaré, 2010; Montange and Batey, 2006; Gilbert et al., 2008; Lu et al., 2008; Stoddard et al., 2010; Wilson et al., 2011) and mechanistically (Garst et al., 2011; Breaker 2012; Haller et al., 2011). Rationally designed SAM analogs to target the SAM-II riboswitch aptamer have been described (Ham et al., 2011), and *S*-2,6-diaminopurinylmethionine was shown to bind the SAM-III riboswitch aptamer (Ottink et al., 2010). However, while the SAM-I riboswitch class has been specifically proposed as an antibacterial drug target (Blount and Breaker, 2006), it has posed a challenge to existing screening methodology.

In this study, we set out to design fluorescently tagged SAM analogs for use in a ligand displacement assay for targeting SAM-I riboswitches (Figure 1A). A fluorescence-based assay was recently developed for the purine riboswitch using 2-aminopurine as the fluorescent ligand, and has considerable advantages over other methods such as in-line probing and isothermal titration calorimetry (Daldrop et al., 2011). Fluorescent SAM analogs based on 2-aminopurine have been prepared (Ottink et al., 2010); however, it is known that the 6-amino group is important for SAM-I riboswitch binding affinity (Lim et al., 2006). Instead, we considered developing fluorescently tagged SAM analogs via installation of a functionalizable linker at different positions.

Analysis of the three-dimensional crystal structures of the SAM-I riboswitch aptamer bound to SAM (Montange and Batey, 2006, Lu et al., 2010) suggested the 2′ and 3′ ribose hydroxyl groups of SAM **1** as candidate positions for fluorophore attachment. Although numerous SAM analogs have been prepared for use as protein substrates or inhibitors, there is currently only one example of chemical modification at the 2′ or 3′ hydroxyl of the ribose moiety (Li et al., 2011). In this work, we report the synthesis of SAM analogs containing functionalized linkers installed onto the 2′ and 3′ ribose hydroxyls and show that these analogs retain binding to the SAM-I riboswitch. We further describe the development of a fluorescence polarization assay using a fluorescently tagged SAM analog for targeting SAM-I riboswitches. We demonstrate a fluorescent ligand displacement assay for targeting SAM-I riboswitches, including the *Staphylococcus aureus metK* SAM-I sequence, that may be useful as a high-throughput screening method for antibacterial drug discovery.

RESULTS

Synthesis and Evaluation of Two Functionalizable SAM Analogs

For targeting SAM-I riboswitches, we sought to develop a synthetic route that was amenable to the installation of functionalizable linkers on the SAM ribose hydroxyl groups. The riboswitch aptamer makes extensive contacts to both the nucleobase and amino acid moieties of SAM **1** (Montange and Batey, 2006, Lu et al., 2010), and functional group transformations at these positions are not well tolerated (Lim et al., 2006). However, the 2′ and 3′ ribose hydroxyls of SAM **1** are located within a solvent-accessible cavity, and only the 2′ hydroxyl is directly contacted through hydrogen bonding interactions (Figure 1B).

Therefore, we designed two prototype analogs **2** and **3** containing either a 2′-3′-O-acetal or 3′-O-propionate linker, respectively (Figure 2A). We based our design on a stable sulfone analog of SAM **1** (SAH sulfone, **4**) that has been shown to bind the SAM-I riboswitch from the *yitJ* transcript of *B. subtilis* with high affinity (K_d value of ~30 nM; Lim et al., 2006). The electropositive character imparted on the sulfur atom by oxidation to the sulfone leads to a higher affinity relative to *S*-adenosylhomocysteine (SAH, **5**), which has a K_d value of ~400 nM (Lim et al., 2006). Thus, we reasoned that fluorescently tagged versions of **4** would be useful in competition binding assays to identify novel riboswitch ligands.

It was envisioned that linkers first could be introduced to the adenosine nucleoside followed by coupling to the homocysteine portion. The 2-(methoxycarbonyl)ethylidine group has been described as an unusually stable acetal protecting group for 1,2-diols (Ariza et al., 2000). As previously shown for 5′-O-trityluridine (Ariza et al., 2000), acetal formation was achieved cleanly by reacting 5′-chloroadenosine **6** with methyl propiolate and DMAP. Because formation of the acetal is nonstereoselective, we isolated and carried forward both diastereomers of **7** (60:40 R/S, diastereomers assigned by NOESY and ratio determined by ^{1}H nuclear magnetic resonance [NMR]).

Thioether formation was effected by coupling **7** with Boc-L-homocysteine following a procedure developed in our lab for efficient preparation of SAH **5** and other analogs (unpublished data). These conditions also led to hydrolysis of the methyl ester. Oxidation of the thioether to the sulfone using urea-hydrogen peroxide and trifluoroacetic anhydride (Balicki, 1999) followed by trifluoroacetic acid deprotection yielded the 2′-3′-O-acetal linked analog **2**. Thus, in addition to stability to strong acid and methanolysis (Ariza et al., 2000), we have shown that this acetal is stable to aqueous base even at slightly elevated temperatures and mild oxidation conditions. Some depurination was observed during acid deprotection, contributing to the relatively low yield of the last step. Unfortunately, we were unable to adequately separate the two diastereomers by HPLC, so the binding analysis was performed on the mixture.

In the X-ray crystal structure of the *B. subtilis* 118 *yitJ* SAM-I riboswitch aptamer, the 2′ hydroxyl of SAM **1** is observed to make two hydrogen bonds, one with the ribose sugar moiety of residue C48 and the other with the O2-carbonyl of residue

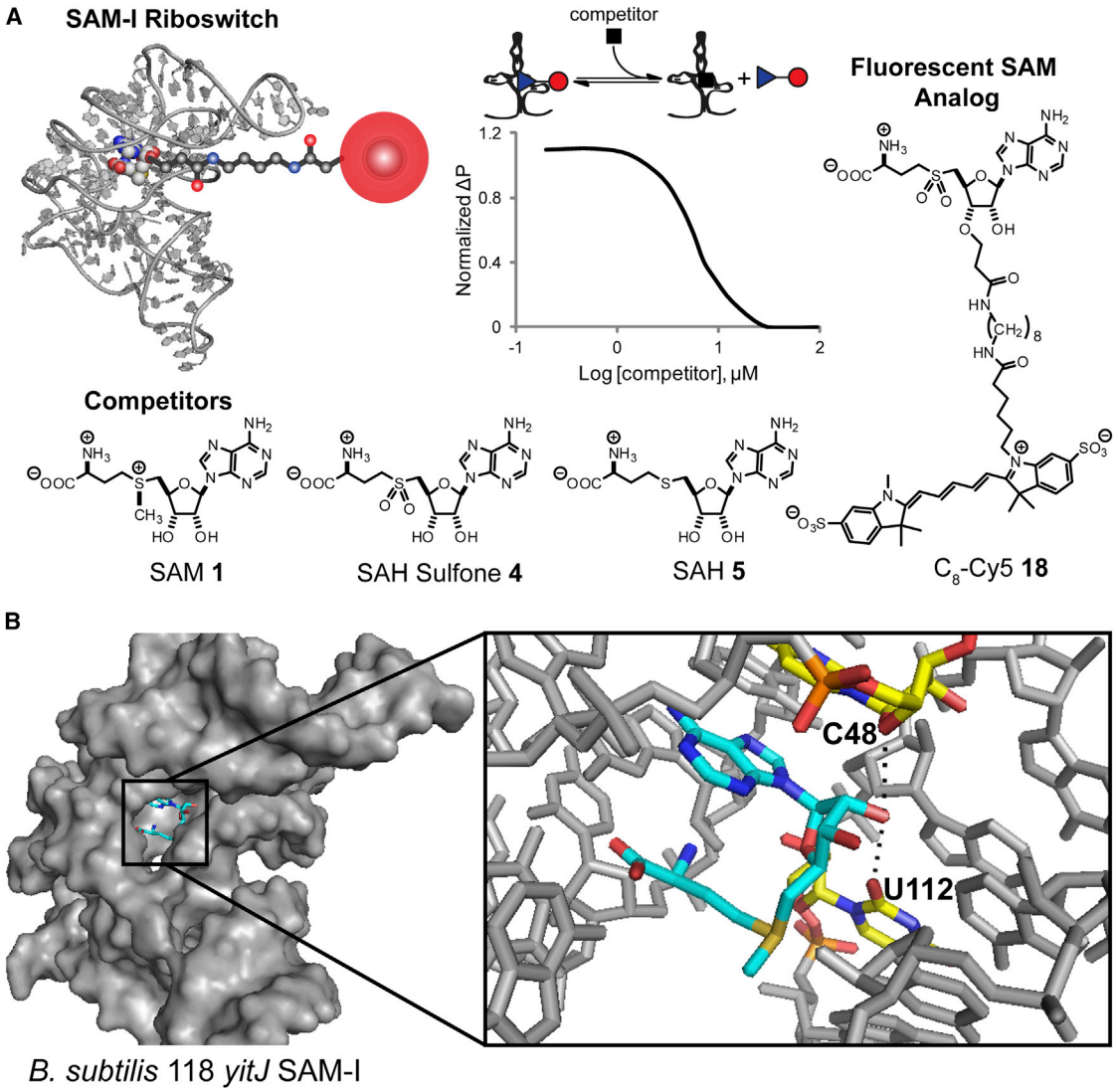

Figure 1. Structure-Based Rational Design of a Fluorescently Tagged Ligand Analog that Targets the SAM-I Riboswitch

(A) Schematic representation of a fluorescent ligand displacement assay for the SAM-I riboswitch. Fluorescent SAM analog is displaced by unlabeled competitor, leading to decrease in fluorescence polarization in a dose-dependent manner. Chemical structures of SAM **1**, SAH sulfone **4**, SAH **5**, and C_8-Cy5 **18** are shown. (B) The X-ray crystal structure of a *B. subtilis* SAM-I riboswitch bound to SAM (PDB code 3NPB) shows that the SAM ribose hydroxyls are solvent accessible. The 2′-hydroxyl makes hydrogen bonding contacts to C48 and U112 of the riboswitch.
See also Figure S3.

U112 (Lu et al., 2010). The 3′-O-propionate linked SAH sulfone analog **3** is proposed to retain these interactions. Because the synthesis of this analog requires mono-alkylation of the 3′ hydroxyl, we first considered methods for selective protection of the 2′ hydroxyl. It was found that the TIPDS (tetraisopropyldisilyl) group, which masks both 5′ and 3′ hydroxyls (Puffer et al., 2008), was not stable to subsequent reaction conditions. Instead, it was more straightforward to react adenosine with PMB chloride directly (Benito et al., 2008) because the 2′-O-PMB protected product selectively recrystallizes from solution. If desired, the 3′-O-PMB protected product remaining in the filtrate can be recycled back to the starting material, adenosine.

While the 5′ chlorination proceeded smoothly to give **9**, the remaining 3′ hydroxyl group was quite unreactive. To install the 3′-O-propionate linker, the best yields were obtained by running the reaction in neat methyl acrylate with *tert*-butoxide. The strong base was added in portions during the course of the reaction to avoid a second alkylation, presumably occurring on the N6 amino group of adenosine, which otherwise leads to a less polar di-alkylated byproduct observed by TLC and LCMS. Under these conditions, we observed preferential alkylation of the 3′ hydroxyl, as the sole mono-alkylated product exhibits a broad singlet integrating to two protons in the ^{1}H NMR spectrum, which is indicative of the N6 amino group. Finally, the 3′-O-propionate linked SAH sulfone analog **3** was obtained from the standard coupling reaction, followed by oxidation to the sulfone and deprotection with acid to remove both Boc and PMB protecting groups.

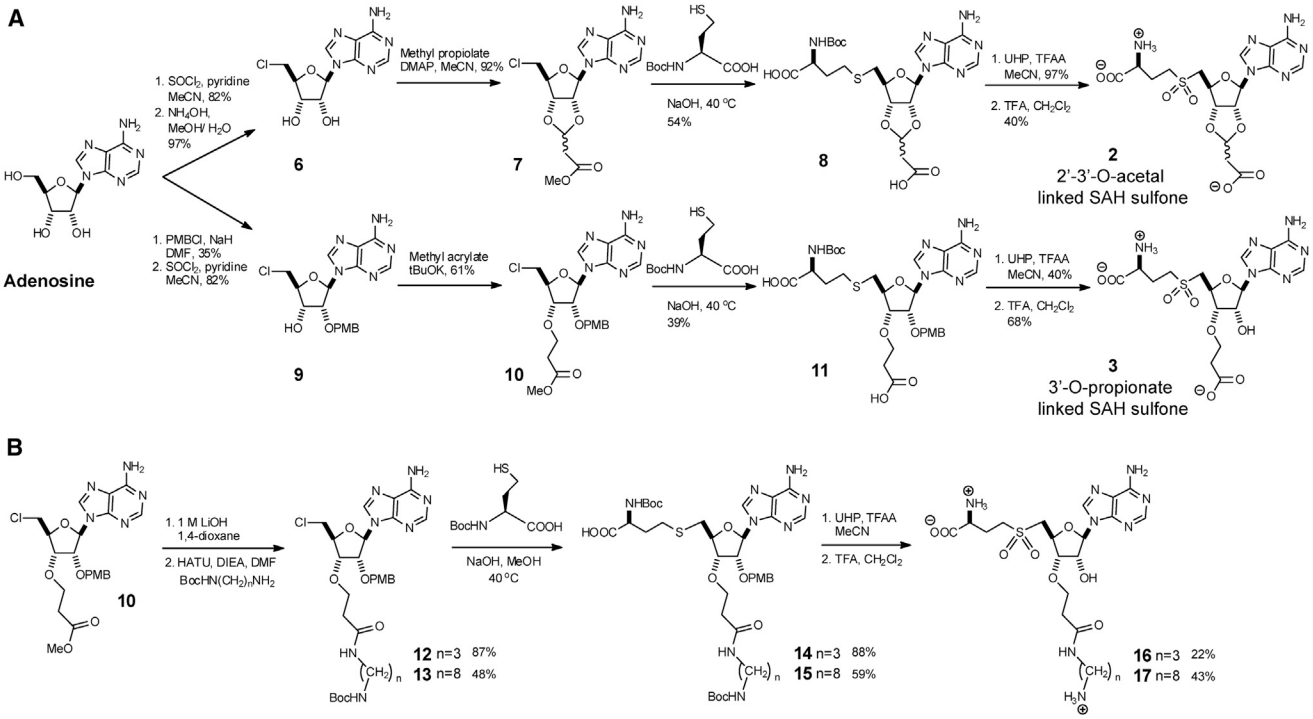

Figure 2. Scheme of Prototype Analogs 2 and 3

(A) Synthetic route to prototype compounds containing 2′-3′-O-acetal (**2**, top) and 3′-O-propionate (**3**, bottom) linkers to SAH sulfone. See also Figure S2.

(B) Synthetic route to C_3 and C_8 linker-containing intermediates **16** and **17**. See also Figure S2.

Compounds **2** and **3** were designed as stable analogs of SAM with two different linkers to probe whether it was possible to functionalize the ligand without blocking binding to the SAM-I riboswitch. Thus, we compared the binding affinities of SAH sulfone **4** and these prototype linker-containing compounds to the *B. subtilis* 124 *yitJ* SAM-I riboswitch aptamer (*Bs* SAM-I; Figure 3A). Dissociation constants for each ligand were determined by performing in-line probing analysis (Regulski and Breaker, 2008) on *Bs* SAM-I in the presence of different concentrations of compound (Figure 3B). The in-line cleavage pattern was identical for all compounds tested and matched that of SAM **1**, with the exception that residue C11 shows increased cleavage in the presence of SAH sulfone **4** and its analogs relative to SAM **1**, consistent with previous observations (Lim et al., 2006). The K_d value for SAH sulfone **4** synthesized using our method (29 nM) matched the previously reported value of 30 nM (Lim et al., 2006).

Furthermore, we found that both **2** and **3** maintain strong binding affinity to the SAM-I riboswitch aptamer. The acetal linker reduces affinity by 4.7-fold (K_d value of ~140 nM). This loss of affinity could be due at least partially to the absence of the 2′ hydroxyl, which is involved in hydrogen-bonding interactions (Figure 1B). In support of this hypothesis, analog **3**, which maintains the 2′ hydroxyl and bears the 3′-O-propionate linker, binds the SAM-I riboswitch aptamer with higher affinity than **2** (K_d value of ~59 nM). While both model compounds **2** and **3** retain binding affinity to the RNA, we considered the 3′-O-propionate linker to be more promising to pursue, because it has little negative effect on binding and does not generate a new stereocenter.

Fluorescently Tagged SAM Analogs Target the SAM-I Riboswitch

To prepare fluorescent analogs, we considered that installing a terminal amine on the 3′ linker would allow us to take advantage of the multitude of commercial amine-reactive fluorescent probes (Figure 2B). Saponification of **10** followed by HATU coupling to either mono Boc-protected 1,3-diaminopropane or 1,8-diaminooctane (Chadwick et al., 2010) gave **12** and **13**, respectively, showing that overall linker length can be modified by simply exchanging the diaminoalkane used in the coupling reaction. The corresponding SAH sulfone analogs were obtained after employing similar thioether formation, oxidation, and deprotection conditions as established for **3**.

Mono protection of the diaminoalkane linker with Cbz also can be effected, but we were concerned with having to perform late-stage deprotection of this group in the presence of a thioether. As the Fmoc protecting group likely is not stable to the conditions for thioether formation, the Boc-protected diaminoalkanes were used. Thus, the final deprotection of **14** and **15** removed both Boc groups and revealed two potentially reactive amines. Efforts to couple to the fluorophore NHS ester in the presence of copper (II) sulfate to block the amino acid (Wiejak et al., 1999) were unsuccessful. However, the ε-amine of lysine has been shown to react with an NHS ester selectively over the α-amine (Chauhan, 2009), so a similar effect was expected with **16** and **17**. Coupling of 5(6)-carboxytetramethylrhodamine (TAMRA) NHS ester with **16** gave a 70:30 mixture of C_3-TAMRA regioisomers as monitored by HPLC, but with **17**, which has a longer alkyl chain, only the desired regioisomer (C_8-TAMRA)

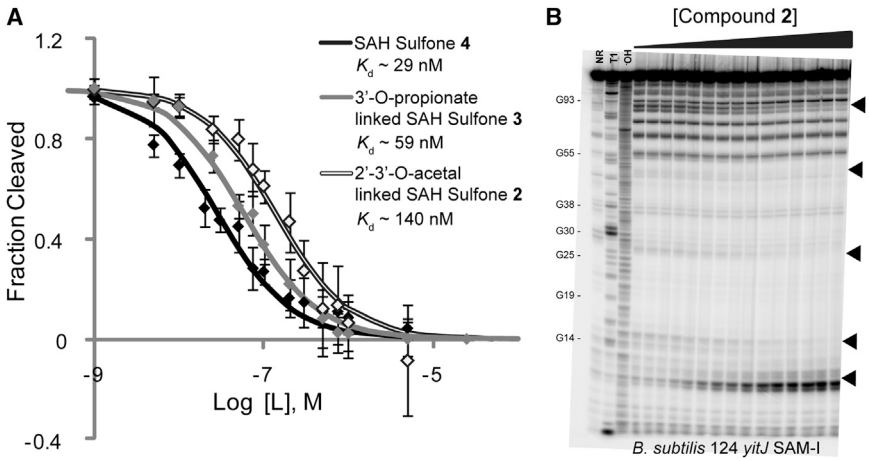

Figure 3. Prototype Linker-Containing Analogs of SAH Sulfone Maintain Affinity for *Bs* SAM-I

(A) Comparison of binding affinities to the riboswitch aptamer for analogs **2** and **3** versus SAH sulfone **4** determined by in-line probing analysis. Data shown are averages for several sites of modulation normalized to the cleavage observed at maximum ligand concentration, or the inverse value (one minus normalized cleavage observed) for sites of increasing cleavage. Also shown are best-fit curves used to calculate K_d values. Error bars represent SD of values for sites of modulation analyzed from a single gel.

(B) Representative in-line probing gel showing change in spontaneous cleavage pattern of *Bs* SAM-I in the presence of **2**. Sites of modulation analyzed are marked by black triangles and several G nucleotides mapped by T1 digest are labeled. NR, no reaction; T1, partial digest with RNase T1; and $^{-}$OH, partial digest with alkali. See also Figure S4.

was observed by HPLC. Assignment of the regiochemistry of C_8-TAMRA was confirmed by correlation to the ^{1}H NMR chemical shifts for the more extensively characterized Cy5-tagged compound **18**.

Other riboswitch-small molecule interactions have been interrogated using a radiolabeled ligand in native polyacrylamide gel electrophoresis (PAGE) (Shanahan et al., 2011). Similarly, binding of the TAMRA-tagged SAM analogs to *Bs* SAM-I was analyzed using native PAGE. Both fluorescently tagged analogs noncovalently labeled *Bs* SAM-I; however, the fluorescent ligand-riboswitch complex was detectable at lower RNA concentrations for C_8-TAMRA (250 nM) than for C_3-TAMRA (5 μM; Figure S1 available online). In-line probing analysis corroborates the native PAGE results (Figure S1), which together suggest that the longer C_8 linker is better tolerated for binding to the riboswitch aptamer.

Coupling of sulfo-Cy5 NHS ester with **17**, which was analyzed by 2D COSY experiments to assign peaks in the ^{1}H NMR (Figure S2), yielded the desired single regioisomer of C_8-Cy5 **18**. Consistent with fluorophore coupling to the C_8 amine linker instead of the amino acid, we observed a decrease in the number of protons attached to the C_8 amine from three to one (Figure S3). In addition, the chemical shift of the adjacent methylene changes from 2.7 to 3.0 ppm (Figure S3), which was also observed for acetylated **16** prepared from mono-acetyl diaminopropane.

Interestingly, the binding affinities of fluorescent ligands C_8-TAMRA (K_d value of ~3 μM) and the related C_8-Cy5 **18** (K_d value of ~2.8 μM) to *Bs* SAM-I (Figure 4A; Figure S1) are similar, in spite of the latter having an additional alkyl spacer. Both exhibit weaker than expected binding to the riboswitch aptamer. This effect is not due to the presence of the linker, as **17** and acetylated **16** both retain relatively strong binding affinities (K_d values of ~142 nM and 102 nM, respectively; Figure S4).

Riboswitch P3 Stem Length Affects Binding of a Fluorescently Tagged SAM Analog

The X-ray crystal structure of the *B. subtilis* 118 *yitJ* SAM-I riboswitch aptamer (Lu et al., 2010) shows that the P3 stem drapes over the solvent-accessible cavity leading to the ribose portion of the ligand (Figures S5A and S5B). Thus, we propose that steric hindrance with the P3 stem due to adding the TAMRA or Cy5 fluorophores to the flexible alkyl linker leads to the observed detrimental effect on riboswitch binding. Alternatively, the fluorophores may affect the conformation of the SAM analog in solution, such that binding to the riboswitch aptamer is less favorable. It also is possible that both factors contribute to the loss in affinity for the fluorescently tagged ligand.

To determine whether the P3 stem contributes to steric clash, we examined three previously characterized SAM-I riboswitch aptamers with varying P3 stem lengths (Figure 4). The published consensus sequence for the SAM-I riboswitch aptamer, which is based on 4757 representative sequences from different bacteria, shows that the length of the P3 stem is highly variable (Barrick and Breaker, 2007). The *Bs* SAM-I riboswitch aptamer has a total P3 stem length of 40 nucleotides, while the 115 nucleotide riboswitch aptamer sequence from the O-acetylhomoserine sulfhydrylase transcript of *Polaribacter irgensii* (*Pi* SAM-I) has a total P3 stem length of 29 nucleotides. Both of these RNAs exhibit similar binding affinities for SAM (K_d values of 4 nM and 3 nM, respectively; Winkler et al., 2003, Karns et al., 2013). In addition, we analyzed the crystallography construct used to obtain the *Thermoanaerobacter tengcongensis* SAM-I riboswitch aptamer structure (*Tt* SAM-I; Montange and Batey, 2006). This 94 nucleotide sequence derived from the *metF* transcript has an artificially shortened P3 stem of 19 nucleotides (Figure S5) and poorer binding affinity for SAM (K_d of 130 nM as determined by isothermal calorimetry; Montange and Batey, 2006).

To deconvolute the effect of sulfone substitution from the effect of the fluorophore tag, the affinities for each riboswitch aptamer to SAH sulfone **4** and fluorescently tagged **18** were measured by the in-line probing assay (Figures 4 and S6). Interestingly, the sulfone substitution had variable effects on binding affinity to the different riboswitch aptamers (Table S1). Comparing the binding affinities for SAM and SAH sulfone, replacement of the sulfonium group with the sulfone leads to similar fold increases in dissociation constants for the *B. subtilis*

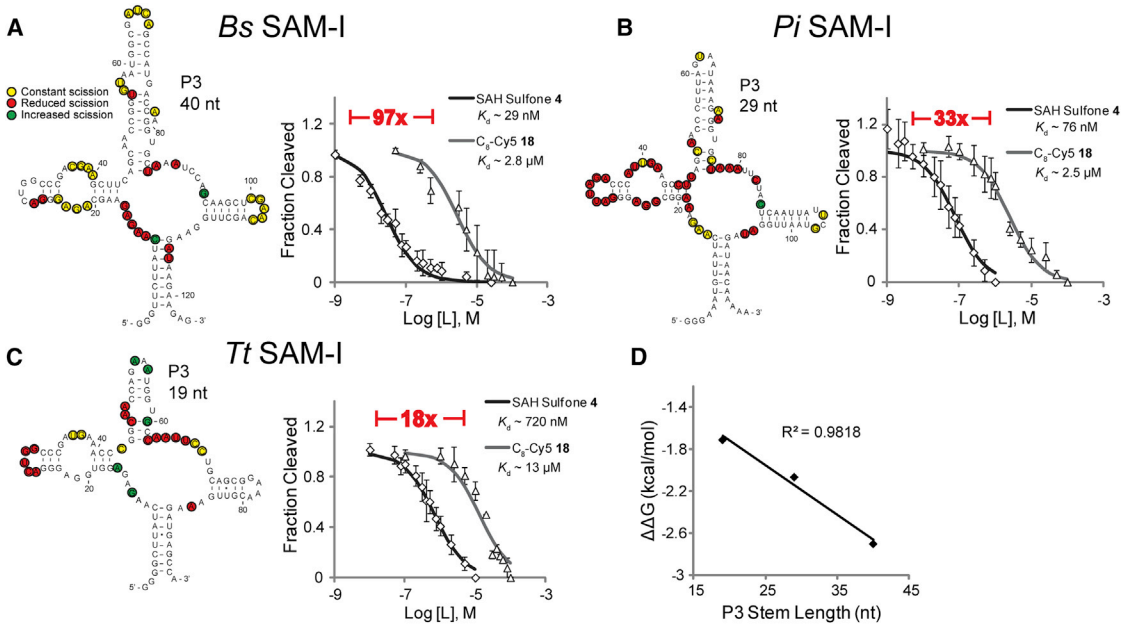

Figure 4. P3 Stem Length Analysis Reveals Major Effect on Relative Ligand Binding Affinity

(A–C) On left, sequences and secondary structure models mapped with in-line probing patterns are shown for (A) *Bs* SAM-I, (B) *Pi* SAM-I, and (C) *Tt* SAM-I. P3 stem lengths are labeled next to each sequence. On right, corresponding in-line probing data and best-fit curves used to calculate K_d values are shown. Error bars represent SD of values for sites of modulation analyzed from a single gel. Relative fold-change in affinity between compounds **4** and **18** is labeled in red.

(D) Plot of the difference in free energy for the dissociation of **18** and **4** versus length of the riboswitch aptamer P3 stem.

See also Figure S6 and Table S1.

and *T. tengcongensis* riboswitch aptamers (7- and 6-fold, respectively). This result matches the observation that the ligand binding pockets for these two aptamers are virtually superimposable (Lu et al., 2010). In contrast, there is a much larger effect of sulfone substitution for the *P. irgensii* riboswitch aptamer (25-fold), but the cause of this is not entirely clear without further structural information. As expected, the effect of the sulfone substitution does not correspond to the P3 stem length, which does not play a direct role in recognition of the sulfonium group (Montange and Batey, 2006; Lu et al., 2010).

In contrast, comparison of dissociation constants for **4** and **18** shows that addition of the fluorophore tag has a detrimental effect on binding affinity that increases with P3 stem length (Figure 4; Table S1). Strikingly, this correlation is linear (Figure 4D), and together with analysis of the two crystal structures (Figure S5) supports the hypothesis that a longer P3 stem may cause steric interference with binding of the fluorescently tagged SAM analog. However, this effect is masked by differences in ligand recognition because the P3 stem also is involved in recognition of the adenosine base of SAM, so the binding affinity of **18** for *Tt* SAM-I is still poorer than that for *Bs* SAM-I. Similarly, we have observed that SAM-I riboswitch aptamers with naturally short P3 stems also exhibit poor binding affinity for **18** (Figures S5C and S5D).

The above results do not eliminate the possibility that addition of the linked fluorophore changes the conformation of the SAM analog in solution. It was previously observed that the fluorescence of flavin adenine dinucleotide is decreased relative to flavin mononucleotide due to the adenine moiety stacking with the isoalloxazine ring (Li and Glusac, 2008). Similarly, we considered that if Cy5 has the propensity to stack with the adenine portion of the SAM analog, one would observe an increase in fluorescence going from this conformation in solution to unstacked upon binding to the riboswitch aptamer. However, there was little difference between the fluorescence intensity of **18** upon addition of water or *Bs* SAM-I (Figure S7), which suggests that binding does not significantly alter ligand conformation. For the same samples, formation of the riboswitch-ligand complex was confirmed by an observed increase in fluorescence polarization (FP).

We further considered that if the fluorescently tagged ligand was prone to aggregation, one would observe an increase in fluorescence polarization upon titration of the ligand. However, while fluorescence intensity increases linearly with respect to compound concentration, the fluorescence polarization was insensitive to changes in ligand concentration up to the value used in binding experiments (Figure S7). The latter observation reveals that the fluorescently tagged ligand is not aggregated under our assay conditions. Thus, these data together suggest that the length of P3 stem of the SAM-I riboswitch affects accommodation of the fluorophore tag attached via the ribose 3′ hydroxyl; however, we cannot rule out that other differences in the aptamer domains contribute to disrupt binding to **18**.

Development of Direct and Competitive Fluorescence Polarization Binding Assays for SAM-I Riboswitches

With the C_8-Cy5 fluorescent ligand **18** in hand, we sought to develop an FP binding assay for SAM-I riboswitches. Previous analysis by the in-line probing assay showed that the fluorescently tagged ligand binds to different SAM-I riboswitch

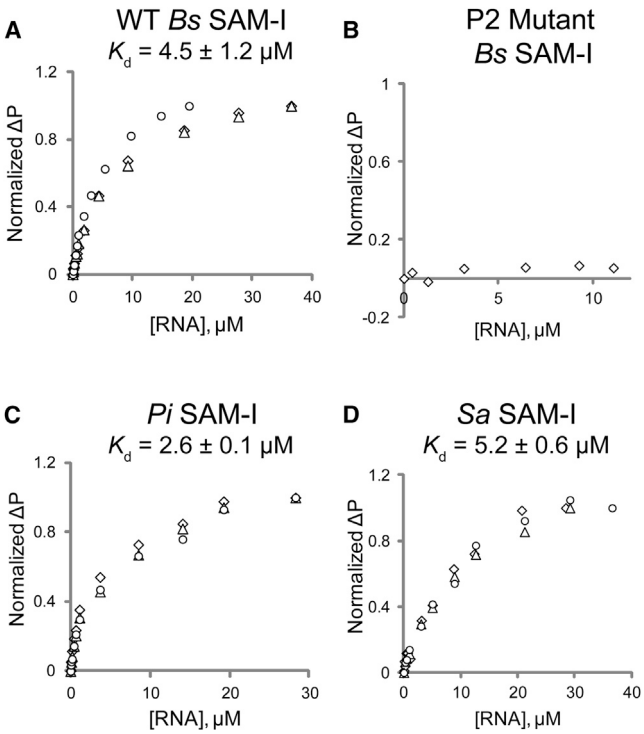

Figure 5. Application of C_8-Cy5 18 to Fluorescence Polarization Binding Assays with Multiple SAM-I Riboswitch Aptamers

Fluorescence polarization of **18** is shown upon titration with (A) WT *Bs* SAM-I, (B) P2 mutant *Bs* SAM-I, (C) *Pi* SAM-I, and (D) *Sa* SAM-I. Different symbols indicate independent replicates. Change in polarization (ΔP) was normalized to the maximal difference observed at the highest RNA concentration. The reported K_d value is the average of those calculated from best-fit curves with margin of error reported as SD.

See also Figure S1.

aptamers (Figure 4). Correspondingly, we observed formation of the riboswitch-ligand complex by increase in FP signal upon titration of the WT *Bs* SAM-I RNA, while no change in FP signal was observed upon titration of a mutant *Bs* SAM-I RNA harboring a disruptive mutation in the P2 stem (Heppell and Lafontaine, 2008; Figures 5A and 5B). Furthermore, the dissociation constants determined from the FP binding assay (4.5 ± 1.2 μM and 2.6 ± 0.1 μM for *Bs* and *Pi* SAM-I, respectively) are in good agreement with those determined by in-line probing assays.

S. aureus is the causative pathogenic agent of a significant portion of hospital-acquired infections (Otto, 2012). The *S. aureus metK* gene encodes *S*-adenosylmethionine synthetase, which has been shown to be essential in *E. coli* (Wei and Newman, 2002) and *B. subtilis* (Kobayashi et al., 2003) and is predicted to be essential in *S. aureus* according to shotgun antisense RNA analysis (Forsyth et al., 2002). The expression of this gene is regulated by a computationally predicted SAM-I riboswitch, which represents a potential target for the development of new antibiotics (Blount and Breaker, 2006). Using the FP binding assay, we found that the *S. aureus* 114 *metK* SAM-I riboswitch aptamer (*Sa* SAM-I) binds to the fluorescently tagged SAM analog **18** with a K_d of 5.2 ± 0.6 μM, which is similar to the dissociation constants determined for the other two SAM-I riboswitches.

We next used **18** to develop a competitive ligand displacement assay for targeting SAM-I riboswitches. The ability of SAH, SAH sulfone, and adenosine to displace **18** from *Bs* SAM-I and *Sa* SAM-I was assayed (Figure 5). The first two compounds are expected to be competitive ligands, and indeed titration of these compounds leads to a decrease in FP signal. In contrast, adenosine does not bind *Bs* SAM-I at concentrations up to 25 μM (Winkler et al., 2003), and our FP results are consistent with it being a non-binder (Figures 6C and 6F). The data were fit to equations for complete competitive binding (Roehrl et al., 2004) and half-maximal inhibitory concentration (IC_{50}) values were calculated for SAH and SAH sulfone using nonlinear regression analysis. The IC_{50} values correlate to but do not match the K_d values for these two ligands (30 and 400 nM, respectively, for *Bs* SAM-I; Lim et al., 2006). The difference is due to the recommended design of competition experiments, in which the starting polarization represents 50%–80% of the maximal value (Kishor et al., 2013). Under these conditions, total RNA concentration is high and the IC_{50} values can be overestimations of the K_d values (Cheng and Prusoff, 1973, Swillens, 1995). Nevertheless, the IC_{50} values for SAH and SAH sulfone with both riboswitch aptamers show the expected trend, which is that SAH is a poorer affinity ligand than SAH sulfone. These results suggest that the fluorescent ligand analog **18** can be used to screen compound libraries for lead compounds that bind to *Sa* SAM-I, a potential antibiotic target.

To further validate that the FP competitive ligand displacement assay can be adapted for high-throughput screening, we determined the Z′ factor for performing the assay in a 384-well plate in place of the single cuvette format. The Z' factor provides a measure of assay quality for high-throughput screening (HTS) and accounts for the dynamic range and well-to-well variation of an assay (Zhang et al., 1999). An excellent HTS assay by industry standards has a Z′ factor between 0.5 and 1.0; however, HTS assays with Z′ factors between 0.2 and 0.5 can still be informative (Zhang et al., 1999).

To determine Z′ factors for the competition assay, 16 well replicates on a 384-well plate containing either no competitor or 100 μM of SAM were evaluated in the presence of *Bs, Sa,* or *Pi* SAM-I and **18** by FP signal. Unfortunately, calculated Z′ values for *Bs* and *Sa* SAM-I were 0.31 and 0.22, respectively (Figures 7A and 7B). We hypothesized that the low Z′ values for these RNAs were attributed to the modest changes in FP signal (ΔmP) for *Bs* and *Sa* SAM-I upon competitive displacement of **18** (61 and 46 mP, respectively, as measured by platereader, similar to the overall signal change observed for the cuvette-based assay; see Table S2). In contrast, the *Pi* SAM-I gave the largest ΔmP upon competitive displacement of **18** (110 ± 22 mP), and consistent with this result, the Z′ value for *Pi* SAM-I was calculated as 0.57 ± 0.01, representing an excellent HTS assay (Figure 7C).

In addition, we evaluated 16 well replicates of two other compounds, SAH sulfone or adenosine, at 100 μM concentrations (Figure 7). Interestingly, at this high concentration, we observe some minimal binding for adenosine to the SAM-I riboswitch aptamers, which is consistent with the cuvette-based assay results (Figures 6C and 6F). While SAH sulfone lies beyond the

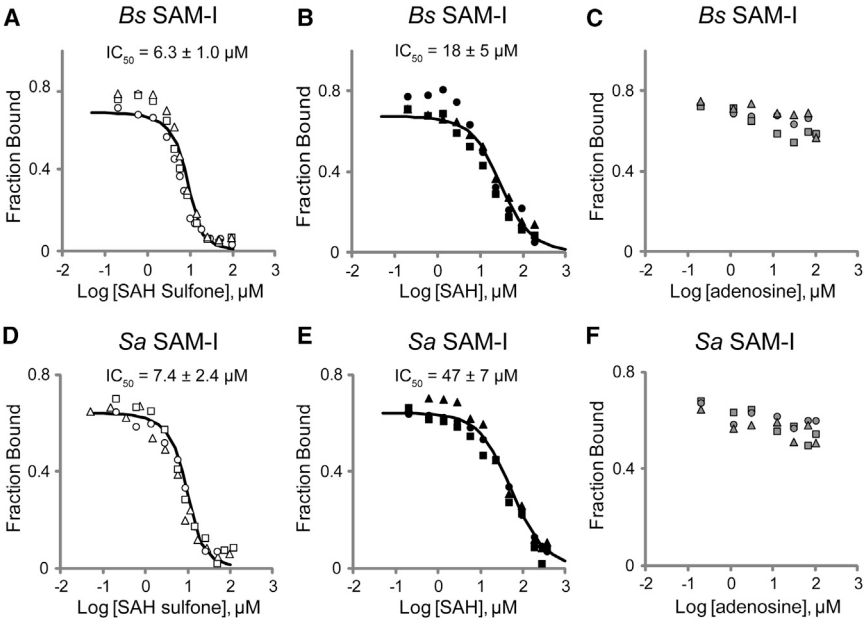

Figure 6. Competitive Ligands Displace C_8-Cy5 18 in a Dose-Dependent Manner as Observed by Fluorescence Polarization

Calculated fraction bound are graphed for **18** upon displacement by SAH sulfone **4** (white boxes), SAH **5** (black boxes), or adenosine (gray boxes) from (A–C) *Bs* SAM-I and (D–F) *Sa* SAM-I. Different symbols indicate independent replicates. The reported IC_{50} value is the average of those calculated from nonlinear regression analysis according to a single-site competition model with margin of error reported as SD.

See also Figure S5.

"no hit" threshold as defined by three SD away from the mean FP signal of the no competitor sample, adenosine does not meet this threshold and represents a non-hit compound. In contrast, SAH sulfone also lies beyond the "hit" threshold as defined by three SD away from the mean FP signal of the positive control, SAM, and so represents a true competitive ligand. Similar ligand binding results are observed for each of the RNAs, but only the assay employing *Pi* SAM-I has a wide signal window for distinguishing between hits and non-hits, as reflected by a demonstrated Z′ factor in the range for a statistically reliable high-throughput screen.

DISCUSSION

Fluorescence polarization has been widely adopted as a high-throughput assay, as screening experiments can be fully automated using commercially available instrumentation (Jameson and Ross, 2010). FP is commonly used for analysis of protein-ligand and protein-nucleic acid interactions (Moerke, 2009) and has been applied to detect metabolite-dependent activation of the *glmS* riboswitch-ribozyme (Mayer and Famulok, 2006). However, prior to our study, it had not yet been explored for standard riboswitch-ligand interactions.

For select riboswitch classes, the cognate ligand has intrinsic fluorescence (Serganov et al., 2009) or can be directly substituted with a fluorescent analog (Budhathoki et al., 2012; Ottink et al., 2010; Daldrop et al., 2011). In each case, it was found that fluorescence is quenched upon binding, and this change in fluorescence has been used to measure ligand binding and competitive displacement. We now have shown that a fluorescently tagged riboswitch ligand can be used for measuring ligand binding via fluorescence polarization. Similar to other fluorescence-based methods, the FP assay enables rapid and direct sample analysis with high sensitivity and without needing a separation step. Furthermore, the reproducibility of the FP signal is increased by its relative insensitivity to changes in fluorophore concentration (Lea and Simeonov, 2011), which improves statistical significance parameters for high-throughput formats. Also, in contrast to assays that rely on changes in fluorescence intensity, ligands can be covalently tagged with a convenient and bright fluorophore at any position that does not disrupt binding. These advantages have made FP-based competition binding assays a workhorse HTS method in the clinical and biomedical fields (Jameson and Ross, 2010), and we expect that it will prove useful for riboswitch-targeted drug discovery as well.

For FP assays, minimal effects on the quantum yield upon binding of the fluorophore are preferable, so the fluorescent tag needs to be placed outside of the ligand binding pocket. It was challenging to rationally design a fluorescently tagged ligand for the SAM-I riboswitch class, because almost every functional group of SAM is recognized by the RNA and the electropositive sulfonium center is hydrolytically unstable. Using two prototype analogs based on SAH sulfone, we explored the possibility of installing a linker to the ribose hydroxyls and found that the 3′ position tolerated functionalization. As planned, fluorophore conjugation to the alkyl amine linker was the last synthetic step, which enables modification of fluorescent properties through choice of the NHS ester reagent (e.g., TAMRA, Cy5) and minimizes the required amount of the expensive fluorophore reagent.

Although RNA-protein interactions typically display larger changes in fluorescence polarization, the FP signal for **18** bound to SAM-I riboswitch aptamers is similar to what has been observed for other RNA-small molecule interactions (Tok et al., 1999). Interestingly, under the conditions of the cuvette-based FP assay, the signal for **18** bound to *Bs* SAM-I is larger than for *Sa* SAM-I (68 versus 43 mP, respectively, see Table S2), in spite of the two RNAs having similar molecular weights and structural folds. Importantly, the dynamic range of the FP signal of **18** was sufficient for determination of K_d and IC_{50} values for ligands and competitors, respectively, for both SAM-I riboswitch aptamers.

To translate the FP competition assay from cuvette-based to 384-well format, we found it necessary to improve the dynamic range of the FP signal for increased statistical significance as measured by the Z' factor. This was accomplished using *Pi* SAM-I, which had a much larger ΔmP (110 ± 22 mP) compared to *Sa* SAM-I (~46 mP). Thus, fluorescently tagged **18** enabled facile screening of multiple SAM-I riboswitch aptamer

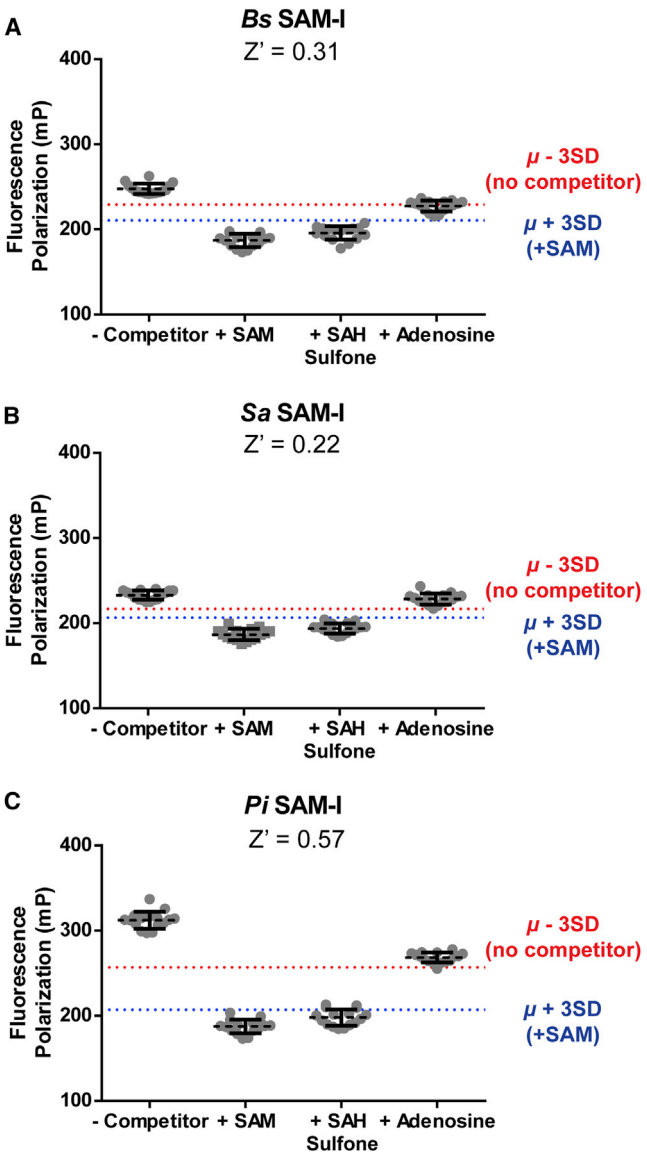

Figure 7. Z′ Values Determined through 384-Well Format Fluorescence Polarization Competitive Ligand Displacement Assay

Fluorescence polarization of **18** graphed for 16 well replicates containing (A) *Bs*, (B) *Sa*, and (C) *Pi* SAM-I with no competitor or 100 μM of SAM, SAH sulfone, or adenosine. The dashed black line indicates the mean (μ) and the solid black bracket indicates the SD for each replicate set. Also shown is the signal window for identifying hits defined by $\mu - 3SD$ for no competitor (red dashed line) and $\mu + 3SD$ for the SAM control (blue dashed line). The Z′ value shown is the average of three plate replicates for *Pi*, or single plate replicates for *Bs* and *Sa*.

See also Figure S7 and Table S2.

sequences for assay optimization. Whereas *Pi* SAM-I itself is not an interesting target for drug discovery, we expect that compounds that bind this RNA found by HTS would be a promising set of candidate ligands for screening against *Sa* SAM-I.

Preliminary hits from a high-throughput binding assay like the one we have developed would need to be further validated, as binding alone does not necessarily confer modulation of the riboswitch regulatory function. However, our assay has the potential to identify compounds that bind within the ligand binding pocket of the riboswitch, as the assay signal is correlated to displacement of the fluorescently tagged SAM analog. Thus there is the strong likelihood of identifying competitor compounds that stabilize the P1 in a manner analogous to the cognate ligand SAM. In addition, two SAM-I expression platforms recently were shown to trigger transcriptional termination in the presence of either theophylline or tetracycline when the expression platforms were fused to the corresponding in vitro evolved aptamer (Ceres et al., 2013). The results from that study suggest that a simple binding event is sufficient to induce regulation through stabilization of the P1 helix. Nevertheless, it is expected that compound leads could be further validated using more low-throughput functional screens, such as the molecular beacon assay (Chinnappan et al., 2013) or the two-piece switching assay recently developed for the *T. tengcongensis metF* SAM-I (Hennelly and Sanbonmatsu, 2011).

In this study, we have demonstrated that there is a signal threshold for adapting FP assays for RNA-small molecule interactions to the HTS format. The FP assay requires optimization of the fluorescently tagged ligand, and we further showed that it may be beneficial to screen related RNA targets in the HTS format. We recommend a practical limit for ΔmP in the 384-well format of above 80 mP when using a manual multichannel pipette because the SD between replicates is typically 10%–15%. However, use of an automated pipetting system should decrease SD to 3%–4% and allow the ΔmP to be considerably lower (~40 mP; Mayer and Famulok, 2006). We expect that these results may inform FP-based HTS screening efforts for small molecule drug candidates against other therapeutic RNA targets in general (Thomas and Hergenrother, 2008).

Although knowledge of the structure of the riboswitch-ligand complex aided in the design of the Cy5-tagged analog **18**, the binding affinity of this compound was poorer than expected given the results for the linker-containing prototype **3**. However, individual members of the SAM-I riboswitch class with higher affinity for **18** may exist. The FP assay readily allows screening for such variants in a riboswitch aptamer library because it does not require chemical modification or labeling of each RNA. Furthermore, additional riboswitch classes that bind SAM as the cognate ligand have been described (Gilbert et al., 2008; Lu et al., 2008; Weinberg et al., 2008) that may bind **18** as well. Experiments for targeting other SAM riboswitch classes are currently in progress.

Additionally, SAM-binding proteins such as histone methyltransferases represent interesting therapeutic targets and have been the focus of drug discovery efforts in recent years. For example, the lysine methyltransferase SET7/9 has generated interest as a drug target for type II diabetes, AIDS, and hormone-dependent breast cancer (Wagner and Jung, 2012). Also, the G9a methyltransferase is upregulated in lung, prostate, and hepatocellular carcinoma (Wagner and Jung, 2012). X-ray crystal structures of each of these enzymes with inhibitor bound suggest that the SAM ribose hydroxyls are solvent accessible when bound to the protein (Protein Data Bank [PDB] codes 4E47 for SET7/9 and 3K5K for G9a) (Liu et al., 2009). Furthermore, hydrogen bonding interactions to the ribose hydroxyls are not conserved in SET domain HMTs (Campagna-Slater

et al., 2011). Whereas SAH sulfone **4** does not inhibit SET7/9 and G9a (Minkui Luo, personal communication), it has been previously shown that these enzymes are inhibited by their byproduct SAH **5** (Ibáñez et al., 2010). Thus, from intermediate **15** of our synthetic route, one could access a fluorescently tagged SAH analog akin to **18** that potentially could be used to identify inhibitor compounds in an FP-based ligand displacement assay that bind in the cofactor binding site, as opposed to the substrate binding site. Such inhibitors would likely be broad spectrum rather than selective inhibitors, which may be desirable for therapeutic development (Wagner and Jung, 2012).

Significance

In conclusion, we have used structure-guided rational design to develop a fluorescently tagged SAM analog that can be used in FP-based screening of compound libraries for binding to SAM-I riboswitches or other relevant SAM-binding RNAs and proteins. Our synthetic route enables facile modification of the ligand and installation of other functional probes such as biotin, terminal alkyne, or a cross-linking agent for synthetic biology and chemical biology applications. Furthermore, we demonstrate the utility of analyzing multiple riboswitch sequences for the development of a statistically reliable FP-based HTS assay for identifying competitive binders. In addition to the ligand tagging approach being generally applicable to target many riboswitches, the adaptation of HTS methodologies to interrogate RNA-small molecule interactions will be critical to efforts to target other therapeutically relevant RNA structures.

EXPERIMENTAL PROCEDURES

Preparation of DNA Constructs

Sequences for all DNA templates and primers used in this study are provided in Table S2. DNA templates corresponding to riboswitch sequences from different organisms were either amplified by PCR from the genomic DNA or from a single-stranded oligonucleotide ordered from IDT. The resulting PCR products were cloned into the pCR2.1-TOPO vector (Invitrogen) following manufacturer instructions and sequence confirmed.

In Vitro Transcription of RNAs

DNA templates containing the extended T7 promoter sequence and two additional G nucleotides for increased transcription efficiency were transcribed in vitro using T7 RNA polymerase (New England Biolabs) at 37°C for 2–3 hr. RNA was purified in a denaturing (7.5 M urea) 6% polyacrylamide gel and was extracted from gel pieces using Crush Soak buffer (10 mM Tris-HCl, pH 7.5, 200 mM NaCl, and 1 mM EDTA, pH 8.0). RNAs were precipitated with ethanol and resuspended in TE buffer (10 mM Tris-HCl, pH 8.0, and 1 mM EDTA). RNA concentrations were measured by the absorbance at 260 nm using a microvolume UV-Vis spectrophotometer (Nanodrop ND-8000). Concentration values were corrected for hypochromicity by measuring the absorbance at 260 nm after hydrolysis with 50 mM sodium carbonate at 95°C for 1–2 hr (S.C. Wilson, D.T. Cohen, and M.C.H., unpublished data).

In-Line Probing Assays

In-line probing analysis was performed following standard procedures (Regulski and Breaker, 2008, see supplemental experimental procedures). The signal intensity for multiple sites of ligand-induced modulation was normalized to the observed value at the highest ligand concentration, and fraction cleaved was taken as the average of the data analyzed for each modulation site. K_d values were determined by fitting the experimental data to a best-fit curve for a 1:1 RNA–ligand complex.

Cuvette-Based Fluorescence Polarization Binding Assays

Fluorescence polarization readings were carried out using a QuantaMaster fluorescence spectrofluorometer (excitation 646 nm, emission 662 nm, Photon Technology International). Samples were prepared in 50 μl of TBM buffer (90 mM Tris base, 89 mM boric acid, and 10 mM $MgCl_2$, pH 7.0) containing 1 μM of C_8-Cy5, and saturation binding experiments were performed with RNA concentrations ranging from 0 to 40 μM. RNA was added successively to the sample cuvette, and concentration values were corrected for added volume. Samples were equilibrated at 30°C for 2 min prior to each FP measurement using tubing connecting the cuvette holder to a water bath.

For competitive ligand displacement assays, samples were prepared in 50 μl of TBM buffer containing 1 μM of C_8-Cy5 and 10 μM of either *Bs* SAM-I or *Sa* SAM-I RNA, corresponding to ~65% fraction bound. Competitor compounds were added successively to the sample cuvette, and concentration values were corrected for added volume. Competitor binding experiments to *Bs* SAM-I were performed with compound concentrations ranging from 0 to 92 μM for **4** and 0 to 272 μM for **5**. For *Sa* SAM-I, the compound concentration ranges were 0–94 μM for **4** and 0–362 μM for **5**. See also Supplemental Experimental Procedures.

384-Well Fluorescence Polarization Competition Assays

For 384-well FP competitive ligand displacement assays, samples were prepared from a master mix of TBM buffer containing 1 μM of C_8-Cy5 and 10 μM of either *Bs*, *Pi*, or *Sa* SAM-I RNA, with no competitor or with 100 μM of SAM, SAH sulfone, or adenosine. A multichannel repeat pipettor was used to manually add 50 μl of samples into 16 replicate wells on a 384-well plate (Corning low volume flat bottom polystyrene nonbinding surface). FP measurements were taken on a Molecular Devices FlexStation 3 Plate Reader at the UCSF Small Molecule Discovery Center.

SUPPLEMENTAL INFORMATION

Supplemental Information includes Supplemental Experimental Procedures, seven figures, and two tables and can be found with this article online at http://dx.doi.org/10.1016/j.chembiol.2014.01.004.

ACKNOWLEDGMENTS

We acknowledge Michelle Arkin and Chris Wilson at the UCSF Small Molecule Discovery Center for assistance with HTS assay development and Minkuo Luo at Memorial Sloan-Kettering for sharing data on the methyltransferase inhibitor study. This work is supported in part by an NIH New Innovator Award (1DP2 OD008677) to M.C.H., a Career Award at the Scientific Interface from the Burroughs Wellcome Fund to M.C.H., the Aldo DeBenedictis fellowship from the UC Berkeley Department of Chemistry to S.F.H., and an NIH Chemistry-Biology Interface Institutional Training Grant (T32 GM066698). The Synthetic Biology Institute is supported by a grant from Agilent Technologies as an industry partner.

Received: August 22, 2013
Revised: December 12, 2013
Accepted: January 3, 2014
Published: February 20, 2014

REFERENCES

Ariza, X., Costa, A.M., Faja, M., Pineda, O., and Vilarrasa, J. (2000). New protecting groups for 1,2-diols (boc- and moc-ethylidene). Cleavage of acetals with bases. Org. Lett. *2*, 2809–2811.

Baird, N.J., and Ferré-D'Amaré, A.R. (2010). Idiosyncratically tuned switching behavior of riboswitch aptamer domains revealed by comparative small-angle X-ray scattering analysis. RNA *16*, 598–609.

Balicki, R. (1999). A mild and efficient procedure for the oxidation of organic sulfides to sulfones by use of urea-hydrogen peroxide/trifluoroacetic anhydride system. Synth. Commun. *29*, 2235–2239.

Barrick, J.E., and Breaker, R.R. (2007). The distributions, mechanisms, and structures of metabolite-binding riboswitches. Genome Biol *8*, R239 1–19.

Batey, R.T. (2011). Recognition of *S*-adenosylmethionine by riboswitches. Wiley Interdiscip Rev RNA *2*, 299–311.

Benito, D., Matheu, M.I., Morère, A., Díaz, Y., and Castillón, S. (2008). Towards the preparation of 2′'-deoxy-2′-fluoro-adenophostin A. Study of the glycosylation reaction. Tetrahedron *64*, 10906–10911.

Blount, K.F., and Breaker, R.R. (2006). Riboswitches as antibacterial drug targets. Nat. Biotechnol. *24*, 1558–1564.

Blount, K.F., Wang, J.X., Lim, J., Sudarsan, N., and Breaker, R.R. (2007). Antibacterial lysine analogs that target lysine riboswitches. Nat. Chem. Biol. *3*, 44–49.

Breaker, R.R. (2011). Prospects for riboswitch discovery and analysis. Mol. Cell *43*, 867–879.

Breaker, R.R. (2012). Riboswitches and the RNA world. Cold Spring Harb. Perspect. Biol. *4*, a003566.

Budhathoki, P., Bernal-Perez, L.F., Annunziata, O., and Ryu, Y. (2012). Rationally-designed fluorescent lysine riboswitch probes. Org. Biomol. Chem. *10*, 7872–7874.

Campagna-Slater, V., Mok, M.W., Nguyen, K.T., Feher, M., Najmanovich, R., and Schapira, M. (2011). Structural chemistry of the histone methyltransferases cofactor binding site. J. Chem. Inf. Model. *51*, 612–623.

Ceres, P., Garst, A.D., Marcano-Velázquez, J.G., and Batey, R.T. (2013). Modularity of select riboswitch expression platforms enables facile engineering of novel genetic regulatory devices. ACS Synth Biol *2*, 463–472.

Chadwick, J., Jones, M., Mercer, A.E., Stocks, P.A., Ward, S.A., Park, B.K., and O'Neill, P.M. (2010). Design, synthesis and antimalarial/anticancer evaluation of spermidine linked artemisinin conjugates designed to exploit polyamine transporters in *Plasmodium falciparum* and HL-60 cancer cell lines. Bioorg. Med. Chem. *18*, 2586–2597.

Chauhan, S.S. (2009). Enantioselective synthesis of (*L*)-Fmoc-α-Me-Lys(Boc)-OH via diastereoselective alkylation of oxazinone as a chiral auxiliary. Tetrahedron Lett. *50*, 6913–6915.

Chen, L., Cressina, E., Leeper, F.J., Smith, A.G., and Abell, C. (2010). A fragment-based approach to identifying ligands for riboswitches. ACS Chem. Biol. *5*, 355–358.

Cheng, Y., and Prusoff, W.H. (1973). Relationship between the inhibition constant (K1) and the concentration of inhibitor which causes 50 per cent inhibition (I50) of an enzymatic reaction. Biochem. Pharmacol. *22*, 3099–3108.

Chinnappan, R., Dubé, A., Lemay, J.F., and Lafontaine, D.A. (2013). Fluorescence monitoring of riboswitch transcription regulation using a dual molecular beacon assay. Nucleic Acids Res. *41*, e106.

Cressina, E., Chen, L., Abell, C., Leeper, F.J., and Smith, A.G. (2011). Fragment screening against the thiamine pyrophosphate riboswitch thiM. Chem. Sci. *2*, 157–165.

Daldrop, P., Reyes, F.E., Robinson, D.A., Hammond, C.M., Lilley, D.M., Batey, R.T., and Brenk, R. (2011). Novel ligands for a purine riboswitch discovered by RNA-ligand docking. Chem. Biol. *18*, 324–335.

de Silva, C., and Walter, N.G. (2009). Leakage and slow allostery limit performance of single drug-sensing aptazyme molecules based on the hammerhead ribozyme. RNA *15*, 76–84.

Deigan, K.E., and Ferré-D'Amaré, A.R. (2011). Riboswitches: discovery of drugs that target bacterial gene-regulatory RNAs. Acc. Chem. Res. *44*, 1329–1338.

Forsyth, R.A., Haselbeck, R.J., Ohlsen, K.L., Yamamoto, R.T., Xu, H., Trawick, J.D., Wall, D., Wang, L., Brown-Driver, V., Froelich, J.M., et al. (2002). A genome-wide strategy for the identification of essential genes in *Staphylococcus aureus*. Mol. Microbiol. *43*, 1387–1400.

Furukawa, K., Gu, H., Sudarsan, N., Hayakawa, Y., Hyodo, M., and Breaker, R.R. (2012). Identification of ligand analogues that control c-di-GMP riboswitches. ACS Chem. Biol. *7*, 1436–1443.

Garst, A.D., Edwards, A.L., and Batey, R.T. (2011). Riboswitches: structures and mechanisms. Cold Spring Harb. Perspect. Biol. *3*, a003533.

Gilbert, S.D., Rambo, R.P., Van Tyne, D., and Batey, R.T. (2008). Structure of the SAM-II riboswitch bound to *S*-adenosylmethionine. Nat. Struct. Mol. Biol. *15*, 177–182.

Haller, A., Soulière, M.F., and Micura, R. (2011). The dynamic nature of RNA as key to understanding riboswitch mechanisms. Acc. Chem. Res. *44*, 1339–1348.

Ham, Y.W., Humphreys, D.J., Choi, S., and Dayton, D.L. (2011). Rational design of SAM analogues targeting SAM-II riboswitch aptamer. Bioorg. Med. Chem. Lett. *21*, 5071–5074.

Hennelly, S.P., and Sanbonmatsu, K.Y. (2011). Tertiary contacts control switching of the SAM-I riboswitch. Nucleic Acids Res. *39*, 2416–2431.

Heppell, B., and Lafontaine, D.A. (2008). Folding of the SAM aptamer is determined by the formation of a K-turn-dependent pseudoknot. Biochemistry *47*, 1490–1499.

Ibáñez, G., McBean, J.L., Astudillo, Y.M., and Luo, M. (2010). An enzyme-coupled ultrasensitive luminescence assay for protein methyltransferases. Anal. Biochem. *401*, 203–210.

Jameson, D.M., and Ross, J.A. (2010). Fluorescence polarization/anisotropy in diagnostics and imaging. Chem. Rev. *110*, 2685–2708.

Karns, K., Vogan, J.M., Qin, Q., Hickey, S.F., Wilson, S.C., Hammond, M.C., and Herr, A.E. (2013). Microfluidic screening of electrophoretic mobility shifts elucidates riboswitch binding function. J. Am. Chem. Soc. *135*, 3136–3143.

Kim, J.N., Blount, K.F., Puskarz, I., Lim, J., Link, K.H., and Breaker, R.R. (2009). Design and antimicrobial action of purine analogues that bind Guanine riboswitches. ACS Chem. Biol. *4*, 915–927.

Kishor, A., Brewer, G., and Wilson, G.M. (2013). Analyses of RNA-ligand interactions by fluorescence anisotropy. Biophysical Approaches to Translational Control of Gene Expression. Biophysics for the Life Sciences *1*, 173–198.

Kobayashi, K., Ehrlich, S.D., Albertini, A., Amati, G., Andersen, K.K., Arnaud, M., Asai, K., Ashikaga, S., Aymerich, S., Bessieres, P., et al. (2003). Essential *Bacillus subtilis* genes. Proc. Natl. Acad. Sci. USA *100*, 4678–4683.

Lea, W.A., and Simeonov, A. (2011). Fluorescence polarization assays in small molecule screening. Expert Opin Drug Discov *6*, 17–32.

Li, G., and Glusac, K.D. (2008). Light-triggered proton and electron transfer in flavin cofactors. J. Phys. Chem. A *112*, 4573–4583.

Li, J., Wei, H., and Zhou, M.M. (2011). Structure-guided design of a methyl donor cofactor that controls a viral histone H3 lysine 27 methyltransferase activity. J. Med. Chem. *54*, 7734–7738.

Lim, J., Winkler, W.C., Nakamura, S., Scott, V., and Breaker, R.R. (2006). Molecular-recognition characteristics of SAM-binding riboswitches. Angew. Chem. Int. Ed. Engl. *45*, 964–968.

Liu, F., Chen, X., Allali-Hassani, A., Quinn, A.M., Wasney, G.A., Dong, A., Barsyte, D., Kozieradzki, I., Senisterra, G., Chau, I., et al. (2009). Discovery of a 2,4-diamino-7-aminoalkoxyquinazoline as a potent and selective inhibitor of histone lysine methyltransferase G9a. J. Med. Chem. *52*, 7950–7953.

Lu, C., Smith, A.M., Fuchs, R.T., Ding, F., Rajashankar, K., Henkin, T.M., and Ke, A. (2008). Crystal structures of the SAM-III/$S_{(MK)}$ riboswitch reveal the SAM-dependent translation inhibition mechanism. Nat. Struct. Mol. Biol. *15*, 1076–1083.

Lu, C., Ding, F., Chowdhury, A., Pradhan, V., Tomsic, J., Holmes, W.M., Henkin, T.M., and Ke, A. (2010). SAM recognition and conformational switching mechanism in the *Bacillus subtilis yitJ* S box/SAM-I riboswitch. J. Mol. Biol. *404*, 803–818.

Mayer, G., and Famulok, M. (2006). High-throughput-compatible assay for glmS riboswitch metabolite dependence. ChemBioChem *7*, 602–604.

Moerke, N.J. (2009). Fluorescence polarization (FP) assays for monitoring peptide-protein or nucleic acid-protein binding. Curr Protoc Chem Biol *1*, 1–15.

Montange, R.K., and Batey, R.T. (2006). Structure of the *S*-adenosylmethionine riboswitch regulatory mRNA element. Nature *441*, 1172–1175.

Mulhbacher, J., Brouillette, E., Allard, M., Fortier, L.C., Malouin, F., and Lafontaine, D.A. (2010). Novel riboswitch ligand analogs as selective inhibitors of guanine-related metabolic pathways. PLoS Pathog *6*, e1000865 1–11.

Ottink, O.M., Nelissen, F.H.T., Derks, Y., Wijmenga, S.S., and Heus, H.A. (2010). Enzymatic stereospecific preparation of fluorescent *S*-adenosyl-L-methionine analogs. Anal. Biochem. *396*, 280–283.

Otto, M. (2012). MRSA virulence and spread. Cell. Microbiol. *14*, 1513–1521.

Puffer, B., Moroder, H., Aigner, M., and Micura, R. (2008). 2′-Methylseleno-modified oligoribonucleotides for X-ray crystallography synthesized by the ACE RNA solid-phase approach. Nucleic Acids Res. *36*, 970–983.

Regulski, E.E., and Breaker, R.R. (2008). In-line probing analysis of riboswitches. Methods Mol. Biol. *419*, 53–67.

Roehrl, M.H.A., Wang, J.Y., and Wagner, G. (2004). A general framework for development and data analysis of competitive high-throughput screens for small-molecule inhibitors of protein-protein interactions by fluorescence polarization. Biochemistry *43*, 16056–16066.

Serganov, A., and Nudler, E. (2013). A decade of riboswitches. Cell *152*, 17–24.

Serganov, A., Huang, L., and Patel, D.J. (2009). Coenzyme recognition and gene regulation by a flavin mononucleotide riboswitch. Nature *458*, 233–237.

Shanahan, C.A., Gaffney, B.L., Jones, R.A., and Strobel, S.A. (2011). Differential analogue binding by two classes of c-di-GMP riboswitches. J. Am. Chem. Soc. *133*, 15578–15592.

Stoddard, C.D., Montange, R.K., Hennelly, S.P., Rambo, R.P., Sanbonmatsu, K.Y., and Batey, R.T. (2010). Free state conformational sampling of the SAM-I riboswitch aptamer domain. Structure *18*, 787–797.

Swillens, S. (1995). Interpretation of binding curves obtained with high receptor concentrations: practical aid for computer analysis. Mol. Pharmacol. *47*, 1197–1203.

Thomas, J.R., and Hergenrother, P.J. (2008). Targeting RNA with small molecules. Chem. Rev. *108*, 1171–1224.

Tok, J.B.H., Cho, J., and Rando, R.R. (1999). Aminoglycoside antibiotics are able to specifically bind the 5′-untranslated region of thymidylate synthase messenger RNA. Biochemistry *38*, 199–206.

Wagner, T., and Jung, M. (2012). New lysine methyltransferase drug targets in cancer. Nat. Biotechnol. *30*, 622–623.

Wang, J.X., and Breaker, R.R. (2008). Riboswitches that sense *S*-adenosylmethionine and *S*-adenosylhomocysteine. Biochem. Cell Biol. *86*, 157–168.

Wei, Y., and Newman, E.B. (2002). Studies on the role of the *metK* gene product of *Escherichia coli* K-12. Mol. Microbiol. *43*, 1651–1656.

Weinberg, Z., Regulski, E.E., Hammond, M.C., Barrick, J.E., Yao, Z., Ruzzo, W.L., and Breaker, R.R. (2008). The aptamer core of SAM-IV riboswitches mimics the ligand-binding site of SAM-I riboswitches. RNA *14*, 822–828.

Wickiser, J.K., Winkler, W.C., Breaker, R.R., and Crothers, D.M. (2005). The speed of RNA transcription and metabolite binding kinetics operate an FMN riboswitch. Mol. Cell *18*, 49–60.

Wiejak, S., Masiukiewicz, E., and Rzeszotarska, B. (1999). A large scale synthesis of mono- and di-urethane derivatives of lysine. Chem. Pharm. Bull. (Tokyo) *47*, 1489–1490.

Wilson, R.C., Smith, A.M., Fuchs, R.T., Kleckner, I.R., Henkin, T.M., and Foster, M.P. (2011). Tuning riboswitch regulation through conformational selection. J. Mol. Biol. *405*, 926–938.

Winkler, W.C., Nahvi, A., Sudarsan, N., Barrick, J.E., and Breaker, R.R. (2003). An mRNA structure that controls gene expression by binding *S*-adenosylmethionine. Nat. Struct. Biol. *10*, 701–707.

Zhang, J.H., Chung, T.D.Y., and Oldenburg, K.R. (1999). A simple statistical parameter for use in evaluation and validation of high throughput screening assays. J. Biomol. Screen. *4*, 67–73.

